Journal of
Micro/Nanolithography,
MEMS, and MOEMS

Nanolithography.SPIEDigitalLibrary.org

Optimized lithography process for through-silicon vias-fabrication using a double-sided (structured) photomask for mask aligner lithography

Tina Weichelt
Lorenz Stuerzebecher
Uwe D. Zeitner

SPIE.

Optimized lithography process for through-silicon vias-fabrication using a double-sided (structured) photomask for mask aligner lithography

Tina Weichelt,[a,*] Lorenz Stuerzebecher,[a] and Uwe D. Zeitner[a,b]
[a]Friedrich-Schiller-Universität, Institute of Applied Physics, Abbe Center of Photonics, Albert-Einstein-Street 15, Jena 07745, Germany
[b]Fraunhofer Institute for Applied Optics and Precision Engineering, Albert-Einstein-Street 7, Jena 07745, Germany

Abstract. Through-silicon vias (TSV) are very important for wafer-level packaging as they provide patterning holes through thick silicon dies to integrate and interconnect devices which are stacked in the *z*-direction. For economic processing, TSV fabrication primarily needs to be cost effective, especially for a high throughput. Furthermore, a lithography process for TSV has to be stable enough to allow patterning on prestructured substrates with inhomogeneous topography. This can be addressed by an exposure process which offers a large depth of focus. We have developed a mask-aligner lithography process based on the use of a double-sided photomask to realize aerial images that meet these constraints. [DOI: 10.1117/1.JMM.14.3.034501]

Keywords: mask aligner lithography; through-silicon vias; photomask fabrication; e-beam lithography.

Paper 15058P received Apr. 17, 2015; accepted for publication Jul. 7, 2015; published online Aug. 13, 2015.

1 Introduction

Mask aligner lithography is a well-established technology for microstructure fabrication. Particularly for micro-electromechanical systems, through-silicon vias (TSV) for 3D-IC, and advanced packaging, mask aligners are a cost effective alternative to projection lithography and an important tool due to easy handling combined with a high throughput. Based on shadow printing, mask aligner lithography has a quite simple principle of operation. A photomask pattern is transferred to wafers coated with photoresist by means of UV exposure. The mask and wafer can either be in direct contact or, in the case of proximity lithography, separated by an air gap in the range of 20 to 200 μm. Contact lithography suffers from contamination, yield problems, and possible damage of the photomask. For this reason, contact lithography is not suitable for mass production. Instead, contact free proximity lithography can overcome these problems. But as the mask-to-wafer distance is increased, the resolution of the patterns transfer is decreased.

In terms of TSV fabrication, the resolution is noncritical; rather, the depth of focus is much more important. TSVs, as already mentioned, are providing the base for integration and interconnection of devices that are stacked in the *z*-direction. In that case, the process needs to be tolerant against prestructured substrates with inhomogeneous topography.

Here, we present a new approach for the lithography process for TSV fabrication. The approach is based on double-sided structured photomasks. It guarantees a high depth of focus while utilizing a proximity distance of 30 μm. In this paper, we describe, in detail, the fabrication of such a photomask, with special emphasis on the front to back side alignment.

*Address all correspondence to: Tina Weichelt, E-mail: tina.weichelt@uni-jena.de

For this purpose, different techniques have been developed and demonstrated. Gruber et al.[1] presented a way to align a photomask to a transparent wafer while they are in (near) contact to each other. For an intended double-sided photomask, adjustments and some effort would be necessary to transfer this technique. Another possibility is to realize the alignment procedure on one substrate, then with a double-sided photomask, such as that demonstrated by Jahns and Däschner.[2] Likewise, we have developed an alignment technique for the orientation of the front and back side patterns.

In an additional fabrication step, alignment makers are generated by diffractive elements using UV exposure. With the successful pattern transfer of a 3×3 via-array, the successful photomask alignment is also demonstrated.

For the usage as well as for the fabrication of the double-sided structured photomask, a homogenous and telecentric illumination is required. Within the last years, mask aligner technology has been further developed. The introduction of a new illumination system called "MO Exposure Optics"[3] has significantly improved light uniformity and ensures a telecentric photomask exposure. Additionally, the possibility of free shaped illumination by choosing a specific angular spectrum for exposure is now possible. This integrated technology is based on microlens-integrators and illumination filter plates (IFPs), which define the different angles of exposure. This opens up new possibilities in the field of advanced mask aligner lithography,[4] for example with optical proximity correction, Talbot-lithography or phase shifting as well as for double-sided photomasks.

The different development steps of the double-sided mask photolithography are presented below: beginning with the design, followed by the fabrication of the photomask, and ending with the final TSV pattern in photoresist. The main focus is on the photomask development. The final etching process is not included in the content of this publication.

2 Double-Sided Photomask Design

Mask aligner lithography usually utilizes binary photomasks. Typically, the wafer-oriented side (front) of the mask is structured. Conventionally, binary amplitude photomasks are used. Light that illuminates the photomask is either reflected (partially absorbed) by a chromium layer or passes the mask through its chromium openings. In addition to a binary amplitude design, a binary phase structure can be added. Therefore, grooves with a predefined depth are etched into the photomask. Such a phase-shifting photomask has been already presented in Ref. 5.

By structuring the back of the mask, light can be preshaped and redirected to the front. By this additional degree of freedom, the illumination of the mask pattern on the front side can be specifically tailored to alter the properties of the transmitted light field. Furthermore, the full intensity of the illumination can be brought to the openings in the mask. Thus, the overall transmission efficiency is improved and shorter exposure times can be achieved. Undesired stray light can be blocked at the mask front side leading to a potential increase in contrast for the exposure. For the double-sided photomask, the binary amplitude design is separated from the binary phase pattern and they are placed on different sides of the photomask. First, the light is mainly affected by the binary phase pattern on the back. The targeted phase shift is achieved by proper surface structuring of the mask substrate.

Light passing the grooves experiences different optical path lengths than the light passing through the nonetched regions. A tailored groove depth causes the E-field phase-shifting in comparison to the nonetched regions.[6] To obtain a phase-shift of $\phi = \pi$, the depth of the grooves can be calculated using the equation

$$d_{\mathrm{PS}} = \frac{\varphi \cdot \lambda}{2\pi \cdot (n_{\mathrm{glass}} - n_{\mathrm{air}})}. \tag{1}$$

The principle of the photomask design is shown in the Fig. 1.

The design of the diffractive phase elements is based on the superposition of different fresnel zone plates (FZP). Each single FZP produces a single spot of 20-μm diameter at a distance of 30 μm behind the photomask. By laterally shifting the single FZP design by a certain distance (in our case 40 and 50 μm) and a following superposition, an array of spots can be produced. Here, the array has been limited to 3×3 elements, because if too many lenses are combined, the performance of each single FZP will decreases and hence the focusing function would not work properly. Each diffractive phase element has a diameter of one millimeter. The larger the field size, the greater the amount of light that can be beneficially redirected.

It is worth mentioning that FZP are usually working as binary amplitude structures, but we integrate them as a binary phase pattern on the back of the photomask. In this way, the power of the light is retained and redirected to the important areas for pattern transfer. The higher the intensities are in the areas of the mask openings, the shorter the exposure time will be. However, with large field sizes, the number of fringes of the FZP increases and their smallest feature size decreases. The smaller the feature sizes are, the more expensive the mask fabrication will be. Since a double-sided mask is already time-consuming in fabrication, the minimal feature size has been limited to 1 μm. This ensures a noncritical fabrication process.

In general, the fabrication error of the e-beam lithography amounts to ± 20 nm. This corresponds to a deviation of 5% of the nominal etch depth of 384 nm. An error of 5% has no influence on the performance of the fresenel zone plate, assuming an etch depth error of 20% causes slight changes in the intensity distribution. The following figures show the consequence of a resulting phase shift error on the simulated aerial image 30 μm behind the photomask.

As obvious in Fig. 2(b), an etch depth error has no influence on the pattern itself, only on the intensity distribution. For the final lithographic pattern transfer, this is not crucial, especially because the etch depth error can be assumed to be smaller than 20%.

In addition to etch depth errors, lateral errors can occur. Basically, the duty cycle error lies in the same magnitude as the etch error: ± 20 nm. This error would partly increase the scattering light and shift 0.04% of the intensity of the used diffraction order to a higher order, hence causing a loss in the intensity distribution.[7] In the assumed ranges, the etch and lateral errors have no significant influence on the final exposures and are negligible.

In contrast, the illumination properties of the exposure are of much more interest for the final pattern realization. As already mentioned in the Sec. 1, the new illumination system[3] of the mask aligner enables a customized selection of

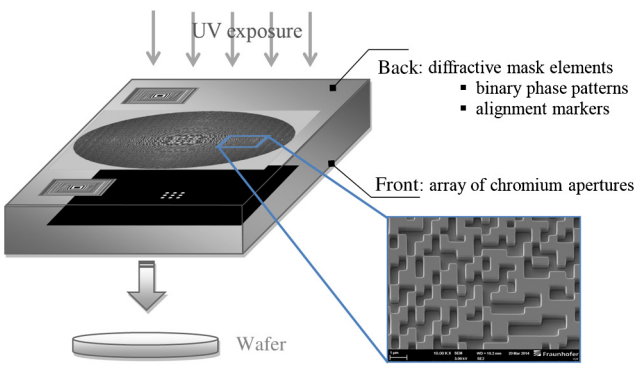

Fig. 1 Layout of the double-sided photomask.

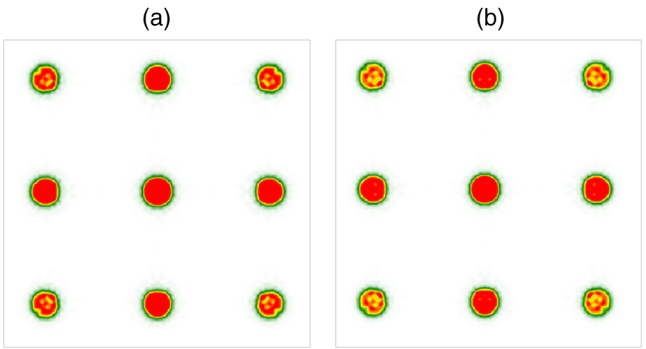

Fig. 2 Simulated aerial image 30 μm behind the photomask, assuming (a) a perfect etch depth of 384 nm and (b) a 20% deviation, causing a phase error and hence a loss in intensity. For both simulations, an angular spectrum of 3 deg was implemented.

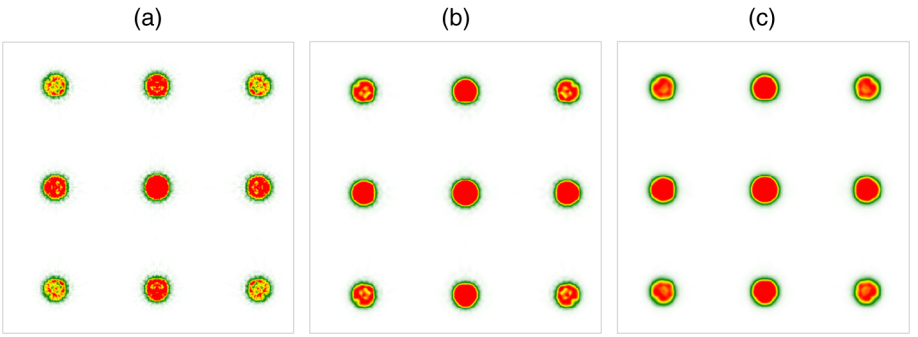

Fig. 3 Influence of different angular spectra on the homogeneity of the aerial image 30 μm behind the photomask. The local period of the array is 50 μm and the diameter of the spots is 16 μm: (a) illumination filter plate (IFP) ⌀5 mm → ±0.2 deg, (b) IFP ⌀40 mm → ±1.7 deg, and (c) IFP ⌀80 mm → ±3.4 deg.

an angular spectrum of the illumination light. Figure 3 visualizes the influence of different applied illumination angles on the aerial image.

It shows that the larger the circular illumination aperture (referred to as IFP) is, the more spatial averaging is generated, thus homogenizing undesired artifacts. Larger IFPs also mean significantly shorter exposure times.

Another benefit of the new "MO Exposure Optics"[3] are multiple microlens arrays, referred to as Köhler integrators that ensure a homogeneity of the illumination in the mask plane better than 3%. For these reasons, no further simulation has been investigated on the imperfection of illumination.

3 Photomask Fabrication

Here, we introduce the fabrication of the double-sided photomask. The following figure summarizes the whole fabrication chain.

The photomask fabrication starts with the structuring of the back of the photomask, as shown in Fig. 4(a). The required photomask pattern was first realized as a resist mask by e-beam lithography and then transferred into the underlying chromium layer by dry-etching. The resulting chromium pattern was then used as a hard-mask for etching the structures into the fused silica substrate. The choice of chromium as the mastering material is to ensure steep sidewalls for the final phase structures in fused silica. The desired depth of 385 nm of the grooves has been determined by the relation of phase-shift and optical path differences in Eq. (1) for the exposure wavelength of $\lambda = 365$ nm.

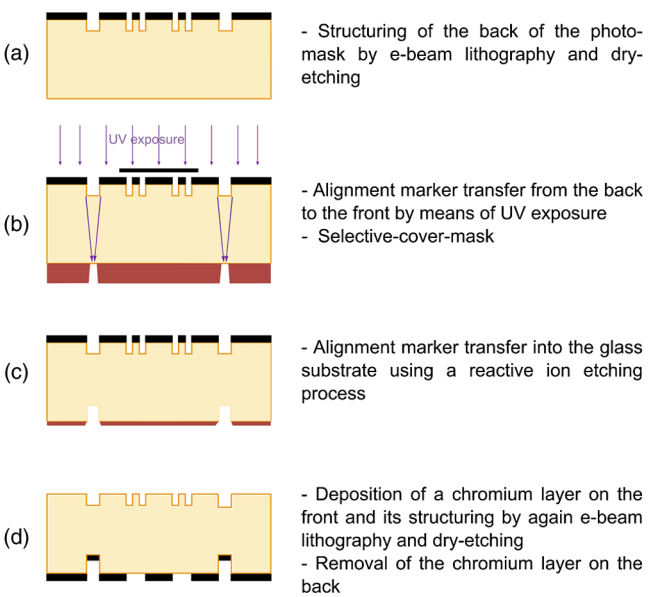

Fig. 4 Technology of a double-sided photomask fabrication.

In the next step [Fig. 4(b)], the generation of the alignment markers is performed. They will be needed for structuring the front side of the photomask. Both patterns of the front and back of the mask need to be well aligned with each other. The alignment markers were first realized in 1-μm thick AZ1505 on the front of the photomask. Therefore, the back of the mask has been exposed with a dose of 0.13 mJ/cm^2 using a SUSS MicroTec Mask Aligner of type MA8Gen3. During the exposure, all other patterns except the alignment markers need to be covered to make sure that no other pattern is copied to the front side of the photomask. The alignment pattern transfer is concluded with etching the photoresist pattern into the fused silica substrate underneath, as sketched in Fig. 4(c). The depth of the marker grooves needs to be at least 300 nm for a later detection in the lithographic patterning process of the front. In Fig. 3, the developmental steps of the alignment markers are shown and will be described below.

The final steps of the photomask fabrication are shown in Fig. 4(d). The front of the photomask is coated with a low-reflective chromium layer. It has a thickness of 96 nm (including a 21-nm chromium oxide layer). This layer is also structured using e-beam lithography. Now the alignment markers that have been etched into the glass substrate can be detected. By the use of such markers, the lithography procedure for the definition of the structures on the front can be aligned to the already existing diffractive elements on the back. Finally, the remaining chromium layer on the back is removed as well. It has been temporarily left there to protect the diffractive phase elements, shown in Fig. 1, during the lithography process for the alignment markers' generation.

As it has been already mentioned, the diffractive elements on the back of the photomask have to be precisely aligned to the circular chrome apertures on the front. Therefore, a special technology has been developed. It ensures an accurate relative alignment, with an accuracy better than 1 μm of structures on both sides of the mask, primarily depending on the feasible pattern detection of the e-beam lithography

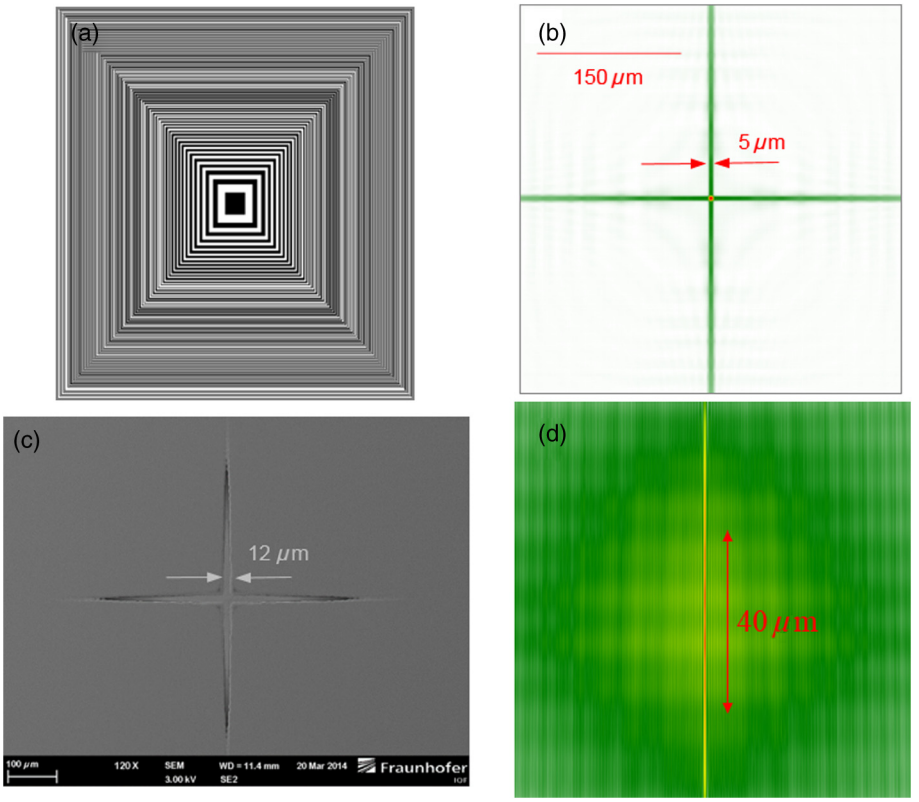

Fig. 5 Cross alignment marker shown as the (a) diffractive binary amplitude pattern, (b) simulating a perfect cross at the front side of the photomask, (d) having a depth of focus about 40 μm. (c) A scanning electron microscope (SEM) image of the realized alignment cross in AZ1505.

for the pattern generation on the second side of the photomask. But, in general, the accuracy is comparable with the one presented in Ref. 2. Different from this and the other mentioned alignment techniques, both the diffractive alignment elements and the binary phase pattern generating the final TSV array are exposed with identical illumination characteristics, reducing illumination errors.

The technology used here is based on special diffractive elements on the back, shown in Fig. 5(a), that are used to transfer the alignment markers to the front of the photomask by means of UV exposure.

In particular, a cross is generated in 1-μm thick photoresist, as it can be seen in Fig. 5(c). A scanning electron microscope image illustrates the alignment marker in the photoresist that will be etched into the fused silica.

The principle of the diffractive elements [Fig. 5(a)] are based on FZP as well, but instead of spherical lenses, patterns for cylindrical lenses are used. As is well known, the greater the number of rings used for FZP, the smaller the achievable focal resolution can be. Our design offers a minimum simulated bar width of 5 μm and a large depth of focus of about 40 μm, as can been seen in Figs. 5(b) and 5(d). The large depth of focus makes the pattern transfer robust against variation of the photomask or the photoresist thickness. In the simulation, the diffractive element has been exposed with an angular spectrum of ± 0.043 deg. In practice, this

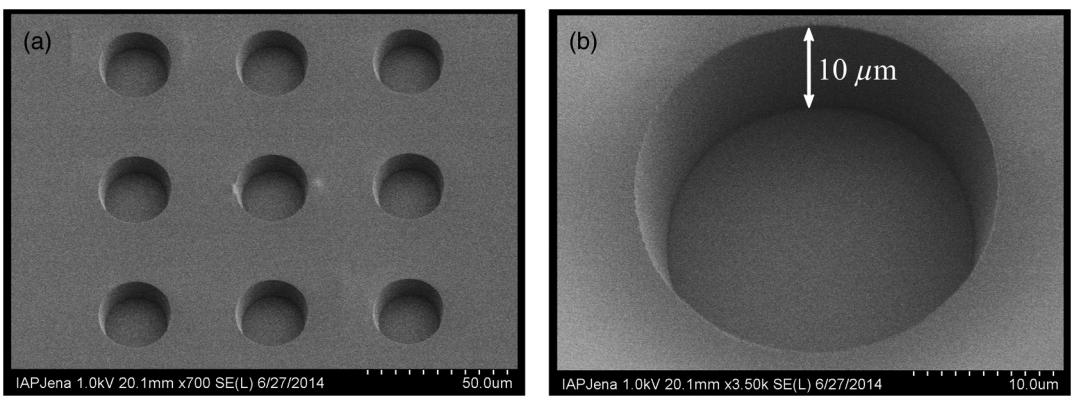

Fig. 6 Photoresist pattern resulting from the mask design in Fig. 1—visualized in a SEM image: (a) as the whole array and (b) as one single via.

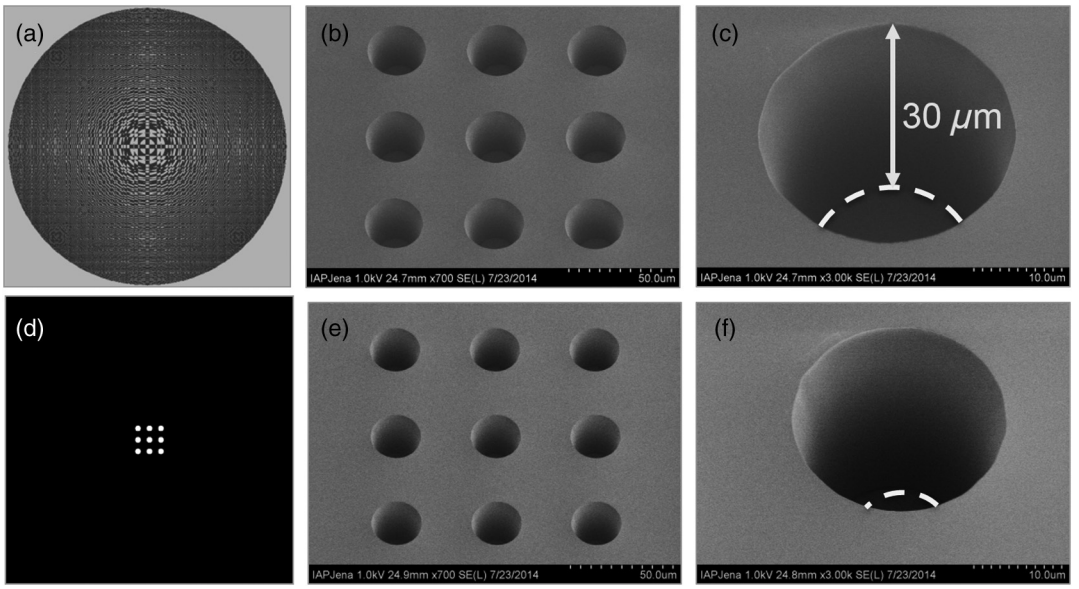

Fig. 7 Pattern transfer into 30-μm thick AZ 9260, based on (a) the binary diffractive element (⌀ 1 mm) on the back of the photomask. (b) and (c) SEM photographs of the full 3×3 via-array with a pitch of 50 μm and its single via. (e) and (f) The photoresist pattern has been achieved with (d) a conventional binary amplitude photomask design.

is transcribed with a circular illumination aperture, referred to as IFP, with a diameter of 0.5 mm. Thus, the achieved trench width of the transferred cross pattern in the photoresist was ~10 μm. The deviation is caused by inaccurate adjustments of the IFP diameter. A larger diameter causes a broader angular spectrum and hence a larger line width. But, in our case, the structure size is still sufficiently small enough for the precise position detection.

4 Experimental Results

The realization of the experiments has been done with the same mask aligner of type MA8Gen3 already used to transfer the alignment markers. The theoretical work has been proofed with the achieved photoresist pattern. For this purpose, we have run different experiments, varying the thickness of the photoresist. For all experiments, a mask-to-wafer distance of 30 μm has been applied.

First, a photoresist (AZ1505) thickness of 500 nm was structured. For the realization, an exposure dose of only 5.5 mJ/cm^2 was necessary. After that, thicknesses of 2 and 10 μm AZ9260 have been structured successfully as well. Figure 6 shows the via-pattern array in a 10-μm thick photoresist.

The pattern transfer into the 10-μm thick resist has been realized by applying an exposure dose of 0.22 J/cm^2. One via-hole has a diameter of 20 μm and the pitch of the presented array is 40 μm. The same pattern has also been successfully transferred onto the 30-μm thick photoresist. These results are shown in Fig. 7.

Figure 7 shows the comparison of photoresist patterns generated with the double sided mask in images (b) and (c) on one hand, and on the other hand, generated with a conventional binary amplitude array (d). The results are shown in Figs. 7(e) and 7(f). The patterns of the conventional mask are located only on the front of the mask.

As a result, the comparison shows steeper sidewalls for the patterns in Figs. 7(b) and 7(c), which were achieved with the double sided photomask. The holes generated with the conventional binary amplitude design are more conic and are not fully opened in the resist. Additionally, the double-sided mask process has been twice as fast as the exposure of the conventional binary photomask. For the structure transfer using the double-sided photomask, an exposure dose of 0.5 J/cm^2 was needed, whereas a dose of 1.05 J/cm^2 was necessary for utilizing a conventional mask.

In a following step of the procedure, the lithographic prepared TSV structure in photoresist can be used to etch the material underneath, e.g., silicon.

5 Conclusion

TSVs have become an important method for wafer-level packaging as they provide patterning holes through thick silicon dies to integrate and interconnect devices which are stacked in the z-direction. The usage of a double-sided photomask enables structuring arrays of holes into thin and thick (500 nm to 30 μm) photoresists applying a mask-to-wafer-distance of only 30 μm. For a reliable pattern transfer, the alignment of the front and back of the photomask needs to be guaranteed. Therefore, special diffractive elements have been developed. The transfer of the final pattern onto the photoresist benefits from short exposure times due to an increased illumination intensity as well as a high contrast and a large depth of focus. The successful alignment of both photomask sides also opens up possibilities for more complex patterns like multilevel structuring. Hence, another degree of freedom can be included and still improve the aerial image, e.g., in contrast, for various application.

Acknowledgments

The authors like to thank all colleagues of the IOF and IAP photolithography clean-room team for the reliable photomask fabrication. Furthermore, the authors appreciate the support of Torsten Harzendorf, providing the SEM images. The presented work was supported by the German Ministry

of Science and Education in the frame of the ultra-optics project "Fertigungstechnologien für hoch entwickelte Mikro-und Nanooptiken" (FZK: 03Z1HN32).

References

1. M. Gruber, D. Hagedorn, and W. Eckert, "Precise and simple optical alignment method for double-sided lithography," *Appl. Opt.* **40**, 5052–5055 (2001).
2. J. Jahns and W. Däschner, "Precise alignment through thick wafers using an optical copying technique," *Opt. Lett.* **17**, 390–392 (1992).
3. R. Voelkel et al., "Advanced mask aligner lithography: new illumination system," *Opt. Express* **18**, 20968–20978 (2010).
4. R. Voelkel et al., "Advanced mask aligner lithography (AMALITH)," *Proc. SPIE* **8326**, 83261Y (2012).
5. T. Weichelt et al., "Resolution enhancement for advanced mask aligner lithography using phase-shifting photomasks," *Opt. Express* **22**, 16310–16321 (2014).
6. M. D. Levenson, N. S. Viswanathan, and R. A. Simpson, "Improving resolution in photolithography with a phase-shifting mask," *IEEE Trans. Electron Devices* **29**(12), 1828–1836 (1982).
7. M. W. Farn and J. W. Goodman, "Effect of VLSI fabrication errors on kinoform efficiency," *Proc. SPIE* **1211**, 125–136 (1990).

Biographies for the authors are not available.